Chapter 4
Structural and Physical Properties of ZnS_xSe_{1-X} Thin Films

Mihail Popa

Abstract ZnS_xSe_{1-x} thin films with various x values in the range from 0 to 1 were prepared by vacuum evaporated technique on glass substrates using powders of ZnS and ZnSe. The structure, surface morphology and composition of thin films have been investigated by XRD, SEM and EDAX techniques. The composition analysis and the diffraction patterns revealed that ZnS_xSe_{1-x} thin films are nearly stoichiometric and have a cubic zinc blende type structure, with a strong orientation of the crystallite along the crystalline plane (111). The temperature dependence of electrical conductivity measured in a temperature range of 300–500 K demonstrated that the films are of n-type conductivity. The thermal activation energy was evaluated from electrical measurements, and the transparency of films in the wavelength range of 380–1100 nm has been demonstrated from oprical measurements. The lifetime of nonequilibrium charge carriers was determined from the relaxation curves of photoconductivity and photoluminescence, and the energy levels of recombination and trapping centers have been determined from the spectral dependence of photoluminescence and thermoluminesce.

4.1 Introduction

The materials for the contemporary optical systems for the visible and infrared wavelength range must have high values of mechanical strength, hardness, high transmission coefficient, optical homogeneity, erosion resistance and thermal stability.

$A^{II}B^{VI}$ wide band gap semiconductor compounds are attractive due to many applications in electronic and optoelectronic nanostructured devices. ZnS and ZnSe polycrystalline semiconductors are perspective materials, which have found many applications in preparing of optical elements working in the visible and infrared. The solid solutions of ZnS_xS_{1-x} ($0 < x < 1$) are much less studied. The interest for

M. Popa (✉)
"Alecu Russo" Balti State University, Balti, Moldova
e-mail: miheugpopa@yahoo.com

© Springer International Publishing Switzerland 2016

I. Tiginyanu et al. (eds.), *Nanostructures and Thin Films for Multifunctional Applications*, NanoScience and Technology,
DOI 10.1007/978-3-319-30198-3_4

the preparation and investigation of physical properties of zinc sulfurselenides is determined by the possibility to vary their physical properties by changing their composition. ZnS_xSe_{1-x} semiconductor materials should combine the high optical characteristics of ZnSe and the mechanical resistance of ZnS. It is interesting to use zinc sulfurselenides as materials for gradient optics.

In the specialized literature there is some information about the use of ZnS_xSe_{1-x} polycrystalline thin films in a variety of optoelectronic applications, such as lasers or laser diodes functioning in the blue spectral range [3] as well as heterojunctions of solar cell [4, 5]. As concerns the environmental protection, ZnS_xSe_{1-x} nanostructured composites are alternative materials for the production of window-layers and buffer-layers for photovoltaic applications, replacing the CdS which is a toxic material [1, 6].

The purpose of this paper is to present the results of research on the structure and surface morphology, electrical, optical and luminescent properties of ZnS_xSe_{1-x} thin films obtained by thermal vacuum evaporation in quasi-closed volume.

4.2 Preparation of ZnS_xSe_{1-X} Thin Films by Thermal Evaporation Method in Vacuum, in Quasi-Closed Volume

Glass substrates of different dimensions (1.5 × 1.5 cm, 1.5 × 3.5 cm and 2.0 × 4.0 cm) were used for the preparation of thin films. During the evaporation they were maintained at different temperatures (300–500 K). For cleaning, the substrates were immersed into a chromic mixture for 24 h. Then, they were removed and rinses with distilled water for several times. To remove traces of salts, the substrates were also rinsed in ethyl alcohol (98 %) and distilled water, and were left to dry.

As a starting material we used powders of ZnSe (with purity 99.9 %) and ZnS (with purity 99.9 %) which were mixed at various concentrations (x = 0, 0.2, 0 4; 0.5; 0.6; 0.8; 1.0).

An automatic installation for thermal vacuum evaporation of UVH-70A-1 type was used for the preparation of thin films. The powder mixtures were poured into tungsten evaporators made in form of a tray. ZnSe and ZnS crystals were deposited onto the substrate by vaporisation (sublimation) of the source material by heating.

ZnS_xSe_{1-x} thin layers with various values of x have been obtained. The substrate-evaporator distance has been modified between 70 and 120 mm. The substrate temperature during deposition varied between 300 and 500 K, and the evaporator temperature varied between 1000 and 1500 K. There were obtained films with thickness between 0.2 and 1.0 μm.

Measurement cells with electrodes in the form of thin films with thicknesses of 1–2 μm were used for the study of temperature dependence of the electrical conductivity (Fig. 4.1a, b). The distance between the electrodes varied between 2–5 mm.

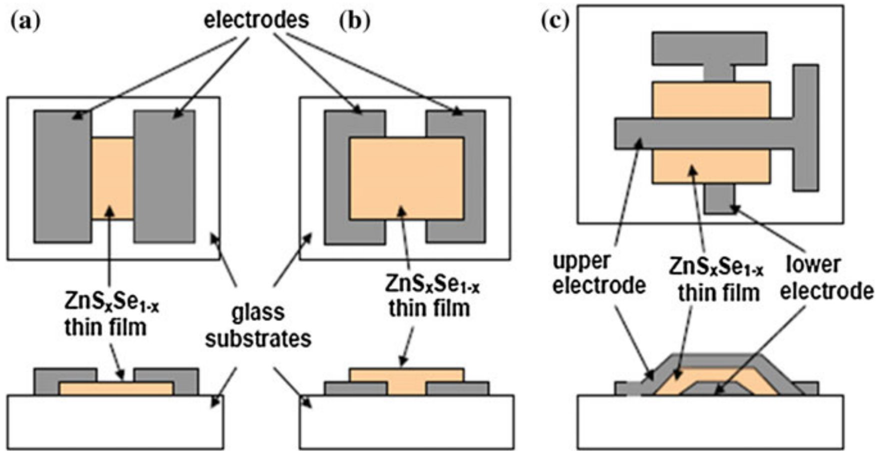

Fig. 4.1 Surface type cells (**a**, **b**) and sandwich type (**c**)

A device with sandwich type cells was used for the study of current-voltage characteristic features (Fig. 4.1c). The sandwich cells were prepared by the deposition of the first In electrode on a glass substrate, followed by the deposition of ZnS_xSe_{1-x} thin films, and finally by the deposition of the second electrode in the direction perpendicular to the first electrode.

4.3 The Structure and Surface Morphology of ZnS_xSe_{1-x} Thin Films

The crystalline structure of the ZnS_xSe_{1-x} thin films was studied by X-ray diffraction using CuK_α radiation (λ = 1.5418 Å). It was found that the layers are polycrystalline and have a cubic structure of zinc blende type, with a strong orientation of the crystallites of the planes (111) parallel to the support surface (Figs. 4.2 and 4.3). The position of this peak deviates from $2\theta = 27{,}297^0$ (for $x = 0$) to the $2\theta = 28{,}612^0$ (for $x = 1$) (Table 4.1).

The parameter of cubic lattice for ZnS_xSe_{1-x} thin films was determined by the relationship [2]

$$a = \frac{\lambda}{2\sin\theta}\sqrt{(h^2 + k^2 + l^2)}, \tag{4.1}$$

where λ is the wavelength of CuK_α radiation (λ = 1.5418 Å) and h, k, l are the Miller indices of the plane (111). The values obtained are in the range a = 5.658 Å (for $x = 0$) and a = 5.406 Å (for $x = 1$) (Table 4.1). Venkata Subbaiah and Ramakrishna Reddy [3] reported similar values of the crystal lattice parameter for similar layers.

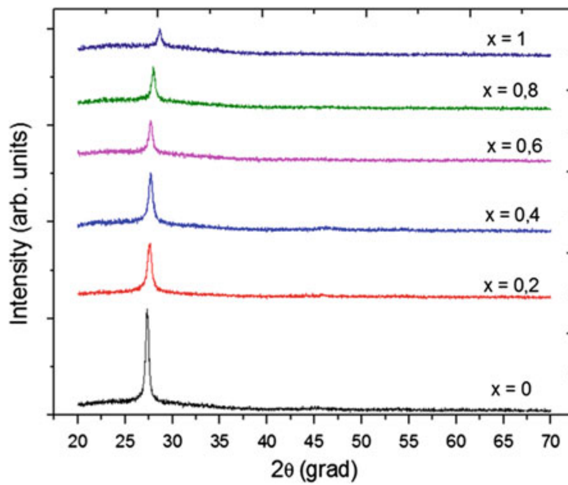

Fig. 4.2 The evolution of diffractograms for ZnS_xSe_{1-x} thin films

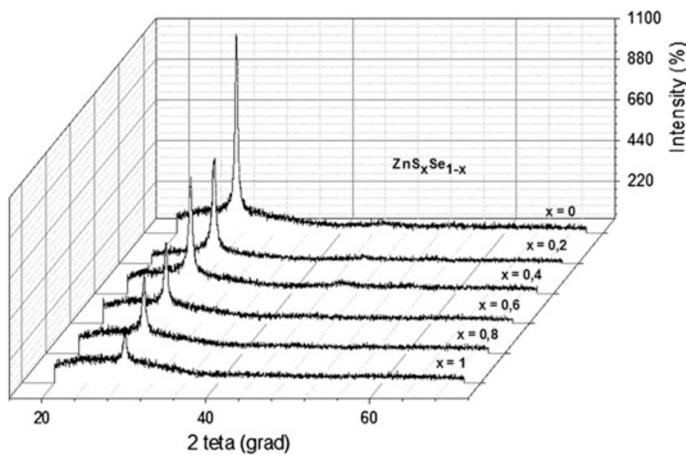

Fig. 4.3 *XRD* analysis for ZnS_xSe_{1-x} thin films

The formula for calculating of the distance between parallel and equidistant planes that have Miller indices (*hkl*) is [2]

$$d_{hkl} = \frac{n\,\lambda}{2\,sin\,\theta}. \tag{4.2}$$

The interplanar distance value for ZnS_xSe_{1-x} thin films was determined using this relationship. The values obtained are in the range of $d_{hkl} = d_{111} = 3.267$ Å (for $x = 0$) and $d_{111} = 3.121$ Å (for $x = 1$) (Table 4.1).

Table 4.1 The experimental values of the cubic structure of ZnS_xSe_{1-x} thin films

x	2θ, grad	*FWHM*	a, nm	d_{111}, nm (*form.* 2)	d_{111}, nm (*form.* 3)
0	27.297	0.4092	5.658	3.267	3.27
0.2	27.423	0.4336	5.634	3.253	3.25
0.4	27.658	0.4654	5.586	3.226	3.23
0.5	27.801	0.4977	5.559	3.209	3.21
0.6	27.952	0.5290	5.529	3.192	3.19
0.8	28.273	0.5663	5.473	3.160	3.16
1.0	28.612	0.6143	5.406	3.121	3.12

The interplanar distance can be calculated directly using the formula for the cubic system [2]

$$d_{hkl} = \frac{a}{\sqrt{h^2 + k^2 + l^2}} \tag{4.3}$$

For the plane (111), we obtain $d_{111} = a/(1^2 + 1^2 + 1^2)^{1/2} = a/3^{1/2}$. By using cubic lattice parameter values, calculated according to the (4.1) we have obtained interplanar distance values between $d_{111} = 3.270$ Å (for $x = 0$) and $d_{111} = 3.120$ Å (for $x = 1$). Venkata Subbaiah et al. [3], Ambrico et al. [4] obtained similar values of interplanar distances for the respective thin films.

The SEM image of ZnS_xSe_{1-x} thin film surface is shown in Fig. 4.4. It is noted that the sample shows small crystallites, and their shape and dimensions are similar. The image indicates the growth of a “columnar” layer (column-shaped crystallites have grown perpendicularly to the support). The roughness of layers determined by scanning electron microscopy is between 2 and 6 nm. The average crystallite size as determined by scanning electron microscopy varied between 3.60 and 2.20 Å.

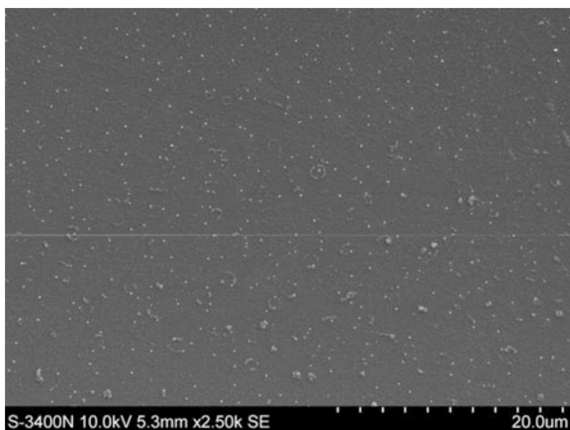

Fig. 4.4 SEM image of $ZnS_{0.2}Se_{0.8}$ thin film

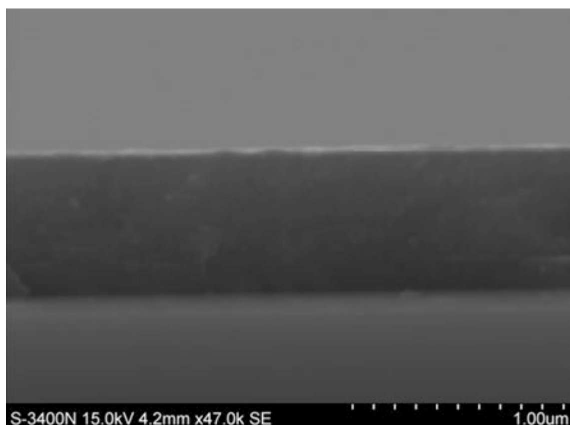

Fig. 4.5 SEM image of fractionated $ZnS_{0.2}Se_{0.8}$ thin film

Figure 4.5 presents the cross-section view of a thin ZnS_xSe_{1-x} layer. It notes that the layer structure is uniform and compact. The thickness of the thin film was determined from this figure.

The EDAX diagrams for ZnS_xSe_{1-x} thin layers are presented in Fig. 4.6, while the initial and the final atomic percentage of chemical elements in the obtained thin layers are shown in Table 4.2. The composition of chemical elements of ZnS_xSe_{1-x} semiconductor compounds is confirmed with an error of about 2–4 %. The presence of a small amount of carbon impurity in the obtained structures is probably due to the amorphous glass substrates which contain this element in their structure.

4.4 The Electrical Properties of ZnS_xSe_{1-X} Thin Films

The study of the influence of temperature on the electrical conductivity of the semiconductor thin films provides information about the conduction mechanisms as well as about possible structural changes that may occur in the layer during the heating process.

The temperature dependence of the electrical conductivity of ZnS_xSe_{1-x} thin films was studied during a thermal treatment consisting of a series of successive heating and cooling processes (temperature rate of 6 K/min) performed in the temperature range of 300–500 K.

The dependencies $ln\sigma = f(10^3/T)$ for some ZnS_xSe_{1-x} polycrystalline thin films (d = 0.15–0.99 μm) are shown in Figs. 4.7, 4.8 and 4.9. The films were prepared by vacuum evaporation method on unheated glass substrate (T_{sub} = 300 K), with the rate of deposition r_d = 1.3–1.6 nm.

A sharp increase of electrical conductivity takes place during the first heating process. During the first cooling and the next cycle of heating and cooling, the curves become reversible and present two distinct parts:

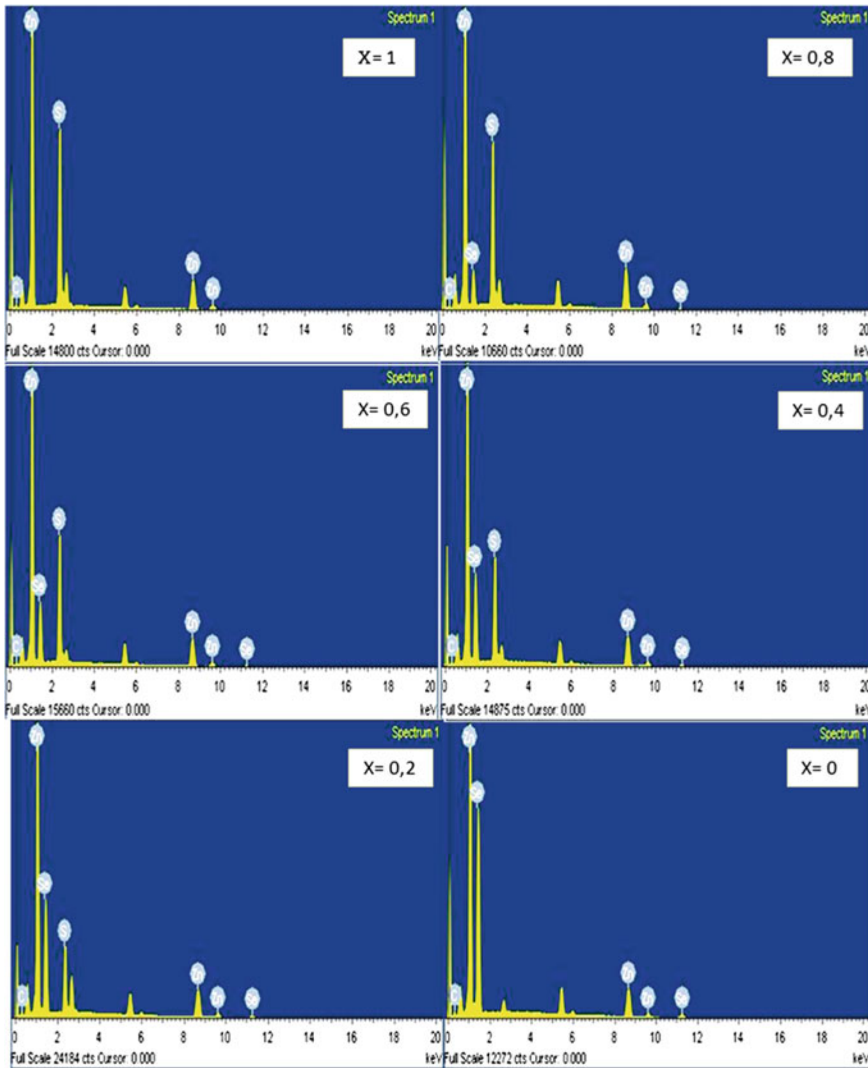

Fig. 4.6 EDAX images for $ZnS_xSe_{1\text{-}x}$ thin films

- the first part in the range of low temperatures suggests that the films exhibit extrinsic conduction;
- the second part in the range of high temperatures corresponds to intrinsic conduction.

Figure 4.10 presents the dependencies $ln\ \sigma = f\,(10^3/T)$ (second heating) for all the films with the values of x = 0; 0.2; 0.4; 0.5; 0.6; 0.8; 1.0. It is observed that with increasing x the conductivity moves to lower values and the slope of this

Table 4.2 Atomic percentage of the elements of EDAX analysis

ZnS_xSe_{1-x}	Zn (%)		S (%)		Se (%)		C (%)
	Teoretic	Exper.	Teoretic	Exper.	Teoretic	Exper.	Experimental
ZnS	50	52.2	50	46.0	–	–	1.8
$ZnS_{0.8}Se_{0.2}$	50	52.0	40	35.9	10	10.1	2.0
$ZnS_{0.6}Se_{0.4}$	50	51.6	30	27.7	20	18.9	1.8
$ZnS_{0.5}Se_{0.5}$	50	51.5	25	22.8	25	23.2	2.5
$ZnS_{0.4}Se_{0.6}$	50	50.9	20	19.1	30	28.2	2.4
$ZnS_{0.2}Se_{0.8}$	50	50.6	10	9.6	40	37.8	2.0
ZnSe	50	50.3	–	–	50	47.1	2.0

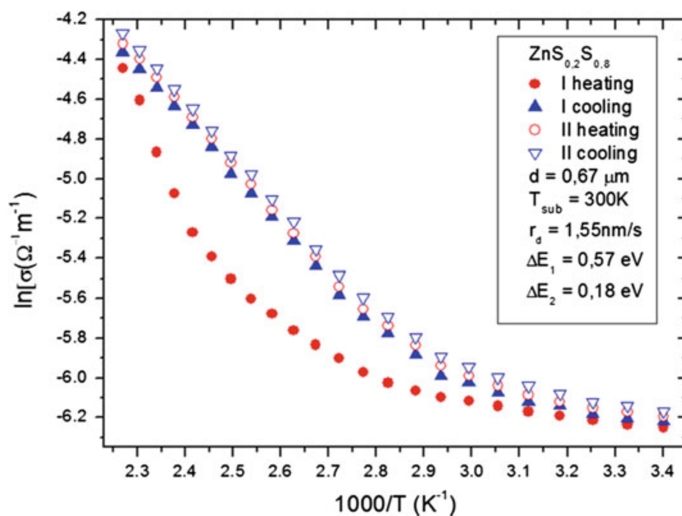

Fig. 4.7 The temperature dependence of the electrical conductivity for $ZnS_{0.2}Se_{0.8}$ sample

dependence increases. The thermal activation energy can be determined from the slope of the curves $ln\ \sigma = f\ (10^3/T)$ in the intrinsic and extrinsic conductivity acording to the relation

$$\Delta E = 0{,}1725 \frac{\lfloor ln\,\sigma_2 - ln\,\sigma_1 \rfloor}{\left(\frac{10^3}{T_1} - \frac{10^3}{T_2}\right)}\ \text{eV}. \tag{4.4}$$

The values of ΔE_1 determined in the field of intrinsic conduction (the temperature range T > 300 K) (Fig. 4.10) vary from 0.43 eV (for x = 0) up to 1.89 eV (for x = 1) (Table 4.3). These values are in good agreement with those found by other authors [3–6].

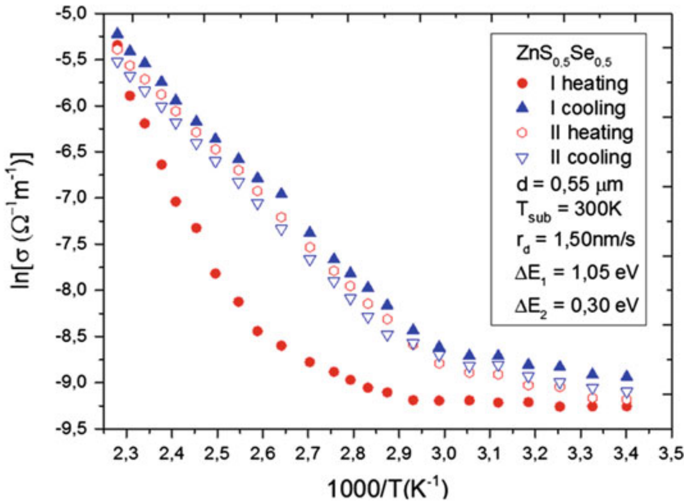

Fig. 4.8 The temperature dependence of the electrical conductivity for $ZnS_{0.5}Se_{0.5}$ sample

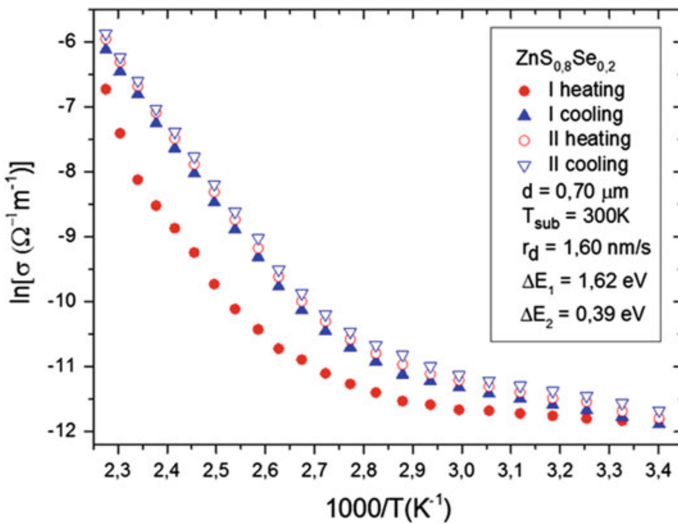

Fig. 4.9 The temperature dependence of the electrical conductivity for $ZnS_{0.8}Se_{0.2}$ sample

The presence of the part related to the extrinsic conduction in the dependencies $ln\sigma = f(10^3/T)$ suggests that additional energy levels located deep within the band gap are present in the studied layers. Interstitial zinc atoms (Zn_i) and selenium vacancies (V_{Se}) are native defects in ZnSe crystals. The energy levels of the Zn_i donor are located below the botom of conduction band (ΔE_d = 0.90 eV) [7], and acceptor levels of V_{Se} are located above the top edge of the valence band

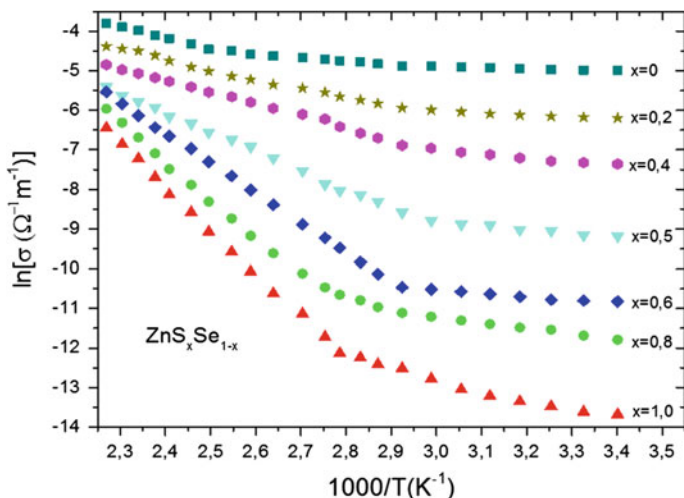

Fig. 4.10 The dependence type lnσ = 10^3/T (II heating) of ZnS_xSe_{1-x} thin films

Table 4.3 The values of thermal activation energy of ZnS_xSe_{1-x} thin films

x	0	0.2	0.4	0.5	0.6	0.8	1.0
ΔE_1, eV	0.43	0.57	0.74	1.05	1.34	1.62	1.89
ΔE_2, eV	0.13	0.18	0.24	0.30	0.34	0.39	0.43

($\Delta E_a = 0.01$ eV) [8, 9]. The shallow impurities (donors and acceptors) are ionized in the temperature range k_BT = 0.026–0.043 eV [8, 9], and the Fermi level is located near the middle of band gap.

From the slopes of the curves $ln\sigma = f(10^3/T)$ in the range of extrinsic conduction (Fig. 4.10), the values of thermal energy activation were determined, ΔE_2, which ranges from 0.13 and 0.43 eV, in the temperature range of T < 300 K (Table 4.3). Probably, these values can be attributed to a complex defect—impurity of the type Zn_i-V_{Se} [7].

Very low values of the thermal activation energy ΔE_2, obtained at low temperature, indicate that the hopping conduction mecanism can be the dominant in these layers, and conduction can be explained on the basis of the Efros-Shklovskii and Mott models for hopping transport in thin layers with high resistance at low temperature [10].

To get new information about the nature of electrical conduction mechanism of thin ZnS_xSe_{1-x} layers, current-voltage characteristics of sandwich systems metal—semiconductor—metal were studied for a large number of samples prepared under different experimental conditions (Fig. 4.1c).

The current-voltage characteristics of the In–$ZnS_{0.5}Se_{0.5}$–In system are shown in Fig. 4.11. Two distinct parts can be distinguished in these charcteristics:

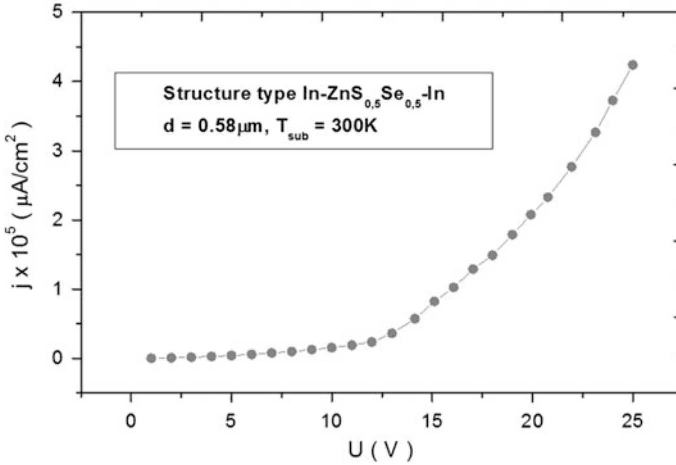

Fig. 4.11 The current-voltage characteristics of structure type In–$ZnS_{0.5}Se_{0.5}$–In

- the first part, which is characterized by a linear dependence of the current intensity upon the applied voltage, and which complies Ohm's law;
- the second part, which has a nearly exponential increase in the intensity of the current with increasing the applied voltage.

If the conduction mechanism is Richardson-Schottky type, current density is expressed by the relationship (4.8, 4.9)

$$I_{RS} = AT^2\left[exp\left(-\frac{\Phi_0}{k_BT}\right)\right]exp\left[\frac{1}{k_BT}\left(\frac{e^3U}{4\pi\varepsilon_0\varepsilon_rd}\right)^{1/2}\right]. \tag{4.5}$$

where A is the Richardson Dushman "effective" constant

$$A = \frac{4\pi m_\theta e k_B^2}{h^2}, \tag{4.6}$$

and Φ_0 is the potential barrier height at the metal-semiconductor interface and m_e is the effective mass of charge carriers.

Logarithm of expression (4.5) gives

$$lnJ_{RS} = ln\left(AT^2\right) - \left(-\frac{\Phi_0}{k_BT}\right) + \left[\frac{1}{K_BT}\left(\frac{e^3U}{4\pi\varepsilon_0\varepsilon_rd}\right)^{1/2}\right]. \tag{4.7}$$

The current-voltage characteristics for the investigated samples, represented in the Schottky coordinates (lnJ, $U^{1/2}$), are also linear. By extrapolating the linear

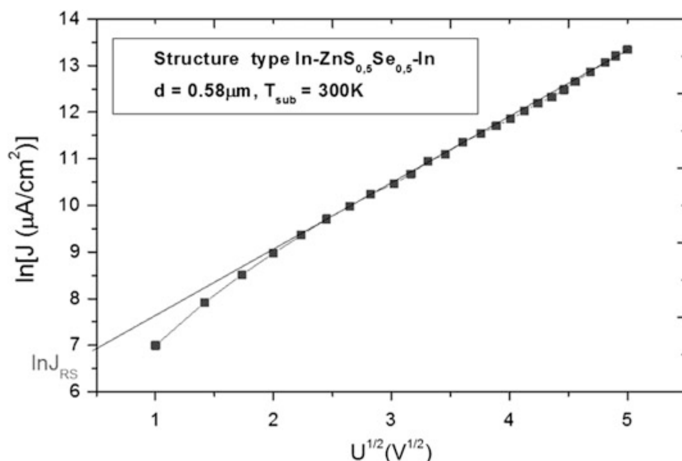

Fig. 4.12 Dependence lnJ = f ($U^{1/2}$) of sandwich system type In–$ZnS_{0.5}Se_{0.5}$–In

segment of the curve $lnJ = f(U^{1/2})$ (Fig. 4.12) for $\sqrt{U} \rightarrow 0$, one can determine the height of the potential barrier at the metal-semiconductor interface

$$\Phi_0 = k_B T \left[ln(AT^2) - lnJ_{RS} \right]. \tag{4.8}$$

Table 4.4 shows some values of Φ_0 calculated for several In–$ZnS_{0.5}Se_{0.5}$–In samples. The values found for Φ_0 correlate well with those found for ZnSe and ZnS crystals [7–9]. This can be explained by the fact that the electrical conduction mechanism is less affected by the contact between crystallites in sandwich systems.

4.5 The Optical Properties of ZnS_xSe_{1-x} Thin Films

The transmission spectrums of the ZnS_xSe_{1-x} thin films have been recorded in the spectral range of 330–1750 nm, using a spectrophotometer Hitachi U-3400.

Table 4.4 The values of potential barrier height of systems type In–ZnS_xSe_{1-x}–In

x	d (µm)	lnJ_{RS} (µA/cm^2)	Φ_0 (eV)
0	0.55	6.20	0.677
0.2	0.67	7.50	0.677
0.4	0.77	8.75	0.678
0.5	0.55	8.50	0.678
0.6	0.50	9.10	0.678
0.8	0.60	8.90	0.679
1.0	0.80	9.30	0.679

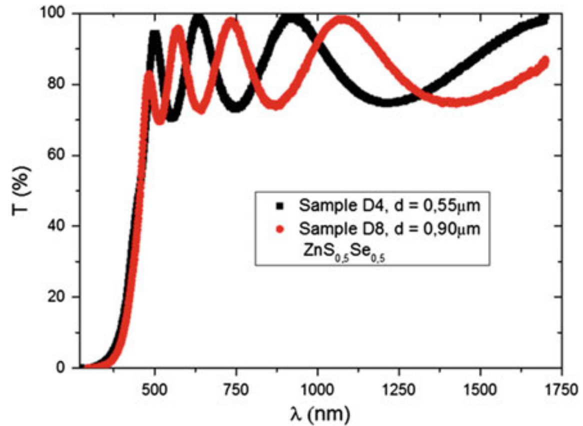

Fig. 4.13 Evolution depending on the thickness of the transmission spectra of $ZnS_{0.5}Se_{0.5}$ thin films

The transmission spectra for two $ZnS_{0.5}Se_{0.5}$ thin films with different thicknesses are shown in Fig. 4.10. The transmission of samples D4 and D8 (Fig. 4.13) increases sharply to a peak value and then decreases slowly in the range of 500–600 nm, after which the evolution of spectra depends on the thickness of samples. Three interference maxima appear in the sample D4 with thickness d = 0.5 μm (Fig. 4.13), while in the sample D8 with thickness d = 0.9 μm there are five maxima. The transmission spectra for the samples with thicknesses greater than 1 μm are formed of a combination of maxima and minima, and the difference between the maximum and minimum transmission decreases with the increase of thin films thickness.

The presence in the transmission spectra of maxima and minima due to the interference of beams reflected at the layer surfaces is an indication that the samples are uniform from the point of view thickness and the layer surfaces are flat. This was also highlighted by the scanning electron microscopy studies (Figs. 4.3 and 4.4), which showed that the roughness of the free surface of the layer is small. A high roughness or irregularity of thickness would lead to the disappearance of interference, namely to the disappearance of minima and maxima in the transmission spectra.

Another analysis was based on the increased concentration of S and the decreased concentration of Se (Fig. 4.14). It is observed that edge transmission spectrum is moving in the lower wavelength region from 420 to 300 nm with increasing the *x* value.

The reflection spectra of ZnS_xSe_{1-x} thin films were measured in the spectral range of 330–1100 nm, using the Hitachi spectrophotometer U-3400. The reflection spectrum of $ZnS_{0.5}Se_{0.5}$ thin films is presented in Fig. 4.12. One can observe that the reflection does not exceed 0.5 % in the wavelength range of 380–1080 nm, while the transmission is between 75–97 % (Fig. 4.15). This tells us that the layers are transparent and the absorption of electromagnetic waves in these layers is also quite small. It is also found that the transmission maxima coincide with the reflection minima, which demonstrates the presence of the interference in the respective films.

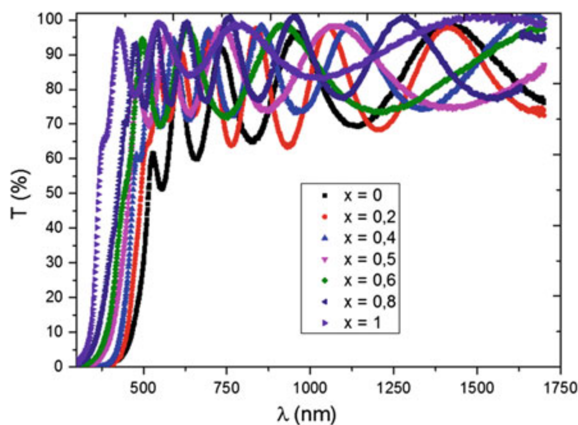

Fig. 4.14 Evolution depending on x of transmission spectra of ZnS_xSe_{1-x} thin films

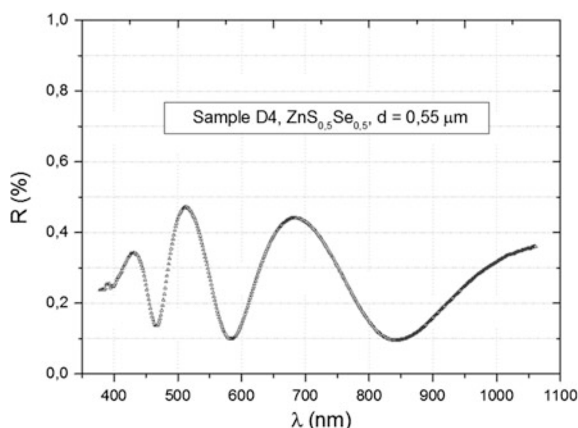

Fig. 4.15 The reflectance spectra of $ZnS_{0.5}Se_{0.5}$ thin films

The absorption coefficient of the ZnS_xSe_{1-x} thin film was calculated from the transmission spectrum (considering the very low reflection of layers) using the formula:

$$\alpha = \frac{1}{d} ln \frac{1}{T}. \tag{4.9}$$

Figure 4.16 presents the absorption spectra of seven polycrystalline ZnS_xSe_{1-x} thin films. It is observed that the absorption edge moves to higher energies from 2.25 up to 3.35 eV with increasing of x value.

In the range of low photon energies, the absorption coefficient has a value different from zero, which can be attributed to the light absorption at the boundaries between crystallites [11]. The high values of the absorption coefficient at photon energies below the fundamental absorption edge may be due to structural defects,

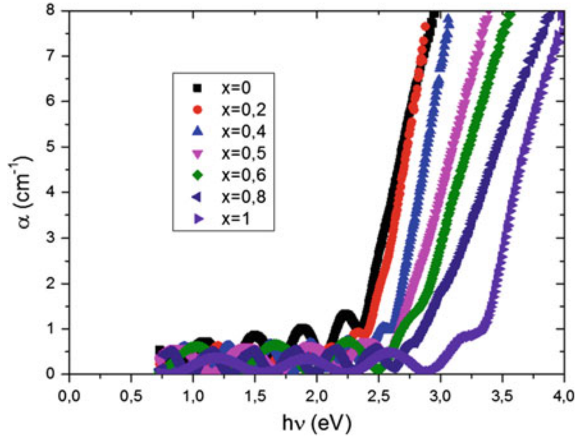

Fig. 4.16 The absorption spectra of ZnS_xSe_{1-x} thin films

which determine the appearance of localized levels in the band gap, leading to electronic transitions as a result of the absorption of incident radiation.

The authors of the paper [11] have explained the form of the absorption spectra by small roughness of the thin film, which leads to the idea of small crystallite size and high degree of crystallization.

For materials with direct band gap we can write the Tauc relationship [11]:

$$\alpha h\nu = A(h\nu - E_g)^{1/2}, \quad (4.10)$$

where A is a constant which is different for different transitions. The presentation of data in coordinates $(\alpha h\nu)^2 = f(h\nu)$ gives a linear dependence. By extrapolating this dependence to $(\alpha h\nu)^2 \rightarrow 0$ one can determine the width of the band gap (E_g) at the given temperature.

The dependencies $\alpha^2(h\nu)^2 = f(h\nu)$ for seven ZnS_xSe_{1-x} thin films are shown in Fig. 4.17. The increase of the thickness of samples leads to increasing the optical absorption and, respectively, the optical band gap deduced from the linear dependence $\alpha^2(h\nu)^2 = f(h\nu)$. The found values of E_g = 2,68–3,50 eV are in good agreement with those established for ZnSe and ZnS crystals [7–9].

Similarly, one can plot the graph

$$\left[h\nu \cdot ln\left(\frac{R_{max} - R_{min}}{R - R_{min}}\right)\right]^2 = f(h\nu), \quad (4.11)$$

where R_{max} and R_{min} are the maximum and minimum of the reflectance spectrum. For the ordinate null value $\left[h\nu \cdot ln\left(\frac{R_{max}-R_{min}}{R-R_{min}}\right)\right]^2 \Rightarrow 0$, the intersection of extrapolated straight line with the ordinate gives the band gap width E_g.

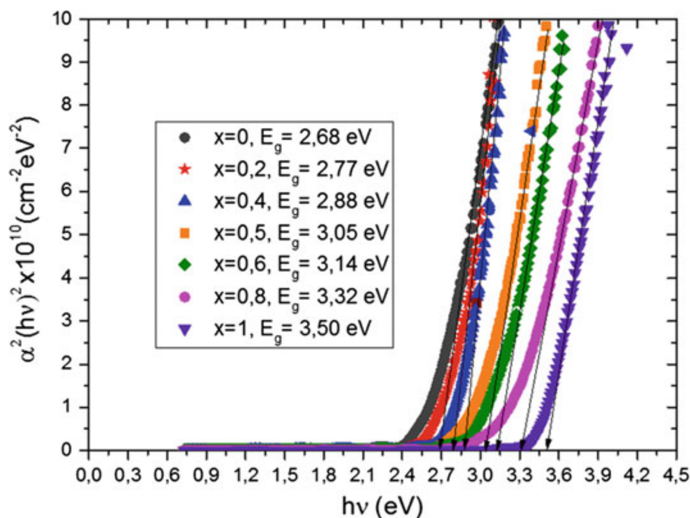

Fig. 4.17 Dependencies $a^2(h\nu)^2 = f(h\nu)$ of ZnS_xSe_{1-x} thin films

The dependencies $\left[h\nu \cdot ln\left(\frac{R_{max}-R_{min}}{R-R_{min}}\right)\right]^2 = f(h\nu)$ for six ZnS_xSe_{1-x} thin films are presented in Fig. 4.18a–f. The values of the band gap between 2.65 and 3.50 eV were obtained by using the method described above.

For comparison, in Table 4.5 are shown the E_g values determined from the reflectance spectra, from absorption spectra and the theoretical values. We note that these values are in good agreement.

The refractive index of the thin film was determined from the transmission spectra using the "envelope" method [12, 13] proposed by R. Swanepoel. The steps of calculating the index of refraction for ZnS_xSe_{1-x} thin films were the following:

(a) Calculation of the refractive index of the substrate, n_s, from its transmission spectrum, $T_{sub} = f(\lambda)$ using the relations [12, 13]

$$n_S = \frac{1}{T_{sup}} - \left(\frac{1}{T_{sup}^2} - 1\right)^{1/2}; \tag{4.12}$$

(b) Plotting windings of interference minima and maxima of the transmission spectrum of a thin film $T = f(\lambda)$ and determining the wavelength for each pair of values T_M and T_m;
(c) Calculation of the coefficient N using the relationship:

$$N = 2n_S \cdot \frac{T_M - T_m}{T_M \cdot T_m} + \frac{n_S^2 + 1}{2}. \tag{4.13}$$

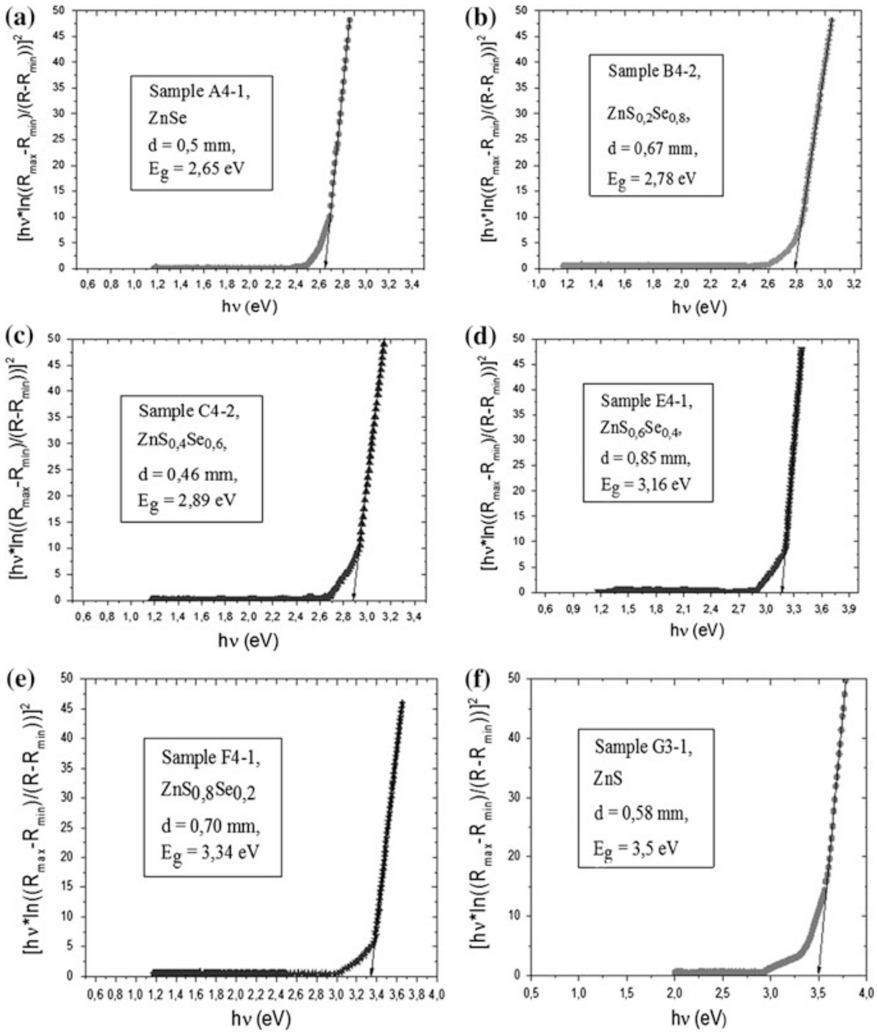

Fig. 4.18 The evolution of width of band gap Eg depending on x for ZnS_xSe_{1-x} thin films

(d) Calculation of *n* values, using the formula:

$$n = \left[N + \left(N^2 - n_s^2\right)^{1/2}\right]^{1/2}, \quad (4.14)$$

The dispersion of the refractive index of ZnS_xSe_{1-x} thin films is presented in Fig. 4.19. Depending on the increase of concentration of S and the decrease of concentration of Se, the refractive index of the respective layers decreases from 2.95

Table 4.5 Comparison of theoretical and experimental values of E_g

Type of semiconductor	Energy band gap, E_g		
	Theoretical	Determined from absorption spectra	Determined from reflection spectra
ZnSe	2.7	2.68	2.65
$ZnS_{0.2}Se_{0.8}$		2.77	2.78
$ZnS_{0.4}Se_{0.6}$		2.88	2.89
$ZnS_{0.5}Se_{0.5}$		3.05	3.06
$ZnS_{0.6}Se_{0.4}$		3.14	3.16
$ZnS_{0.8}Se_{0.2}$		3.32	3.34
ZnS	3.5	3.50	3.50

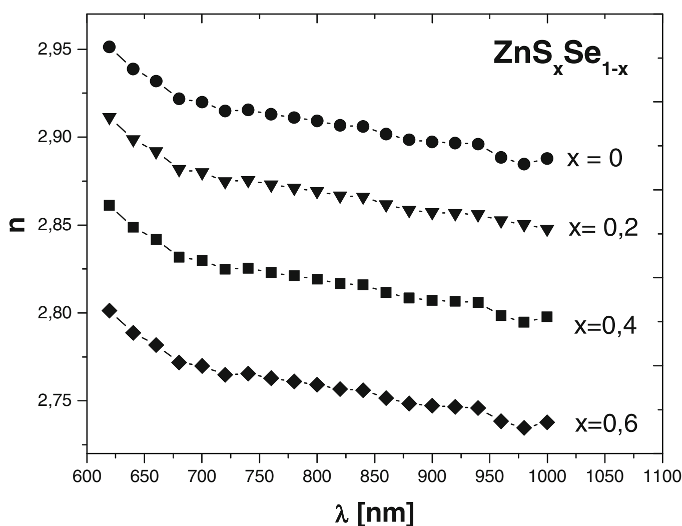

Fig. 4.19 The dispersion of refractive index for ZnS_xSe_{1-x} thin films

(for the sample with $x = 0$) to 2.80 (for the sample with $x = 0.6$). These values are in good agreement with those reported in literature for ZnSe and ZnS crystals [7, 8].

In the frame of a single oscillator model [14], the dispersion of the refractive index in the region of transparency (for photon energies lower than the width of the band gap) can be described by the equation

$$n^2 - 1 = \frac{E_0 E_d}{E_0^2 - (h\nu)^2}, \tag{4.15}$$

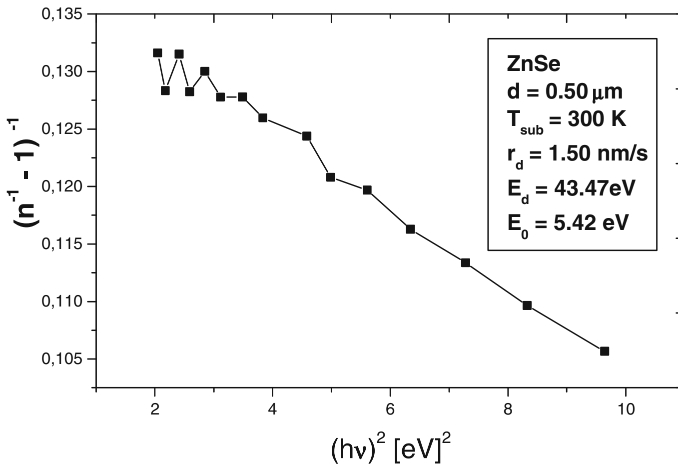

Fig. 4.20 The dependence type 1/(*n*-1 − 1) = *f*(*hv*)2 for ZnSe sample

Table 4.6 Parameters a single oscillator model

ZnS_xSe_{1-x}	Thickness of films d (μm)	Substrate temperature T_{sub} (K)	Deposition rate r_d (nm/s)	E_d (eV)	E_0 (eV)
0	0.50	300	1.50	43.47	5.42
0.2	0.67	300	1.43	45.90	5.56
0.4	0.25	300	1.50	47.35	5.80
0.6	0.50	300	1.60	50.06	6.32
0.8	0.15	300	1.55	52.83	6.70
1	0.50	300	1.55	55.58	6.93

where E_0 is a parameter which value is equal to about double the width of the band gap ($E_0 \cong 2E_g$) and E_d is a dispersion parameter.

Figure 4.20 presents the dependence $1/(n^{-1} - 1) = f(hv)^2$ for ZnSe thin films on the glass. The respective values of E_d and E_0 are obtained from the slope of the linear dependence. The values for other ZnS_xSe_{1-x} thin layers are summarized in Table 4.6.

4.6 The Luminescent Properties of ZnS_xSe_{1-X} Thin Films

In direct band gap semiconductors, such as ZnSe and ZnS crystals, the band to band electronic transitions are vertical and, therefore, for the emergence of intrinsic photoconductivity the incident photon energy *hv* should be equal or larger than the width of the band gap.

For an n-type semiconductor, electrical conductivity caused by the nonequilibrium carriers (photoconductivity) is written as:

$$\Delta\sigma = e\mu_n \Delta n. \tag{4.16}$$

where Δn is the nonequilibrium electron concentration, μ_n is the electron mobility, e is the electron charge.

The decay of the photoconductivity after the light is turn off is desribed for the case of linear recombination by the formula

$$\Delta\sigma = \Delta\sigma_{st} e^{-\frac{t}{\tau}}, \tag{4.17}$$

where $\Delta\sigma_{st}$ is the stationary photoconductivity, τ is the carrier lifetime.

The lifetime characterizes the decrease in the concentration of non-equilibrium carriers, and it is an important parameter in describing the phenomenon of photoconductivity.

Figure 4.21a–e presents the relaxation curves of photoconductivity of $ZnS_{0.5}Se_{0.5}$ thin films measured at different temperatures. Note that the stationary photoconductivity $\Delta\sigma_{st}$ decreases with increasing the sample temperature. This is explained by the fact that the recombination probability ($R \sim \alpha$) is higher at higher temperatures.

The dependencies of $\ln(\Delta\sigma/\Delta\sigma_{st}) = f(t)$ calculated from the relaxation curves of the $ZnS_{0.5}Se_{0.5}$ sample measured at various temperatures are presented in Fig. 4.22. Note that these dependencies are linear. From the slope of these dependencies, the lifetime (τ) of non-equilibrium charge carriers was calculated using the relationship

$$\tau = \frac{t_2 - t_1}{\left(\ln\frac{\Delta\sigma_1}{\Delta\sigma_{st}}\right) - \left(\ln\frac{\Delta\sigma_2}{\Delta\sigma_{st}}\right)}, \tag{4.18}$$

One can see that the value of τ decreases with increasing the sample temperature.

Specialized studies [15] have revealed that the photoconductivity with large relaxation time can be attributed to the presence in the sample of collective potential barriers related to different types of inhomogeneities. The electric field of these barriers produces a separation of the nonequilibrium charge carriers generated by illumination. In such a case, the recombination rate is low, since the probability that an electron will reache a region which contains holes is very low. The phenomenon was revealed in a series of semiconductor $A^{II}B^{IV}$ materials [15, 16].

Figure 4.23 presents the spectral characteristic of photoconductivity for a $ZnS_{0.5}Se_{0.5}$ thin films. The value of $\Delta\sigma/\Delta\sigma_{st}$ is called relative spectral sensitivity and it is given in relative units. This characteristic presents a curve with two peaks localized at 2.33 and 2.54 eV respectively.

The photoluminescence relaxation curve represents the variation with time of the intensity of luminescence, $J_{FL} = f(t)$, after the sample illumination is switched off. It follows the exponential decay law of the form

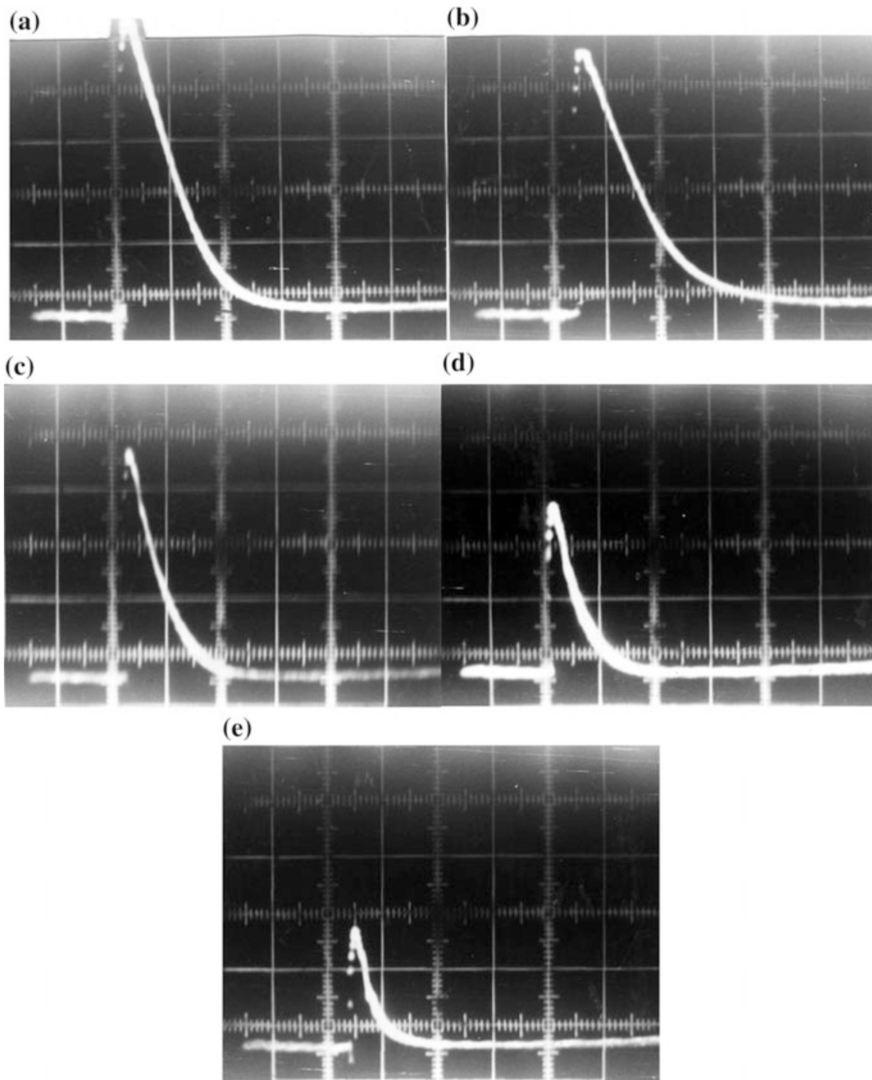

Fig. 4.21 Relaxation curves of the photoconductivity a thin film of $ZnS_{0.5}Se_{0.5}$ (d = 0.55 μm, T_{sub} = 300 K, r_d = 1.50 nm/s) at sample different temperatures (in ordinate indicates $\Delta\sigma = \sigma_L - \sigma_0$ in relative units): **a** T = 81 K (1 cm = 0.1 μs); **b** T = 175 K, (1 cm = 0.2 μs); **c** T = 225 K, (1 cm = 0.2 μs); **d** T = 262 K (1 cm = 0.4 μs); **e** T = 300 K (1 cm = 0.4 μs)

$$J_{FL}(t) = J_{FL}(0)exp\left(-\frac{\mathbf{t}}{\tau}\right), \tag{4.19}$$

where J_{FL} is the luminescence intensity at the momentum of illumination switching off (t = 0), and τ is the lifetime of non-equilibrium carriers.

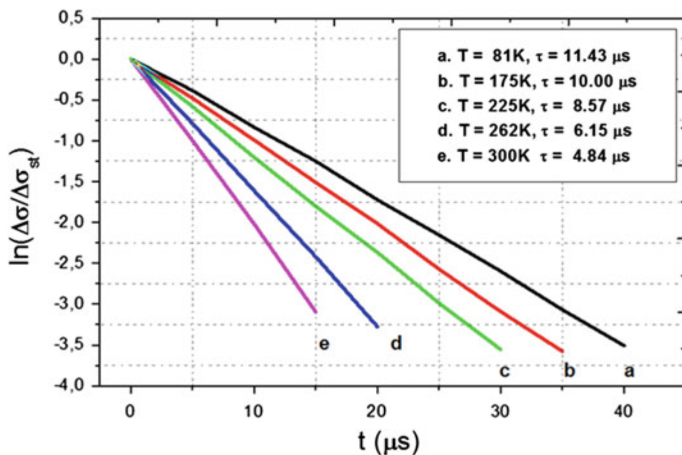

Fig. 4.22 The dependencies $\ln(\Delta\sigma/\Delta\sigma_{st}) = f(t)$ obtained at different temperatures of $ZnS_{0.5}Se_{0.5}$ thin films (d = 0.55 μm, T_{sub} = 300 K, r_d = 1.50 nm/s)

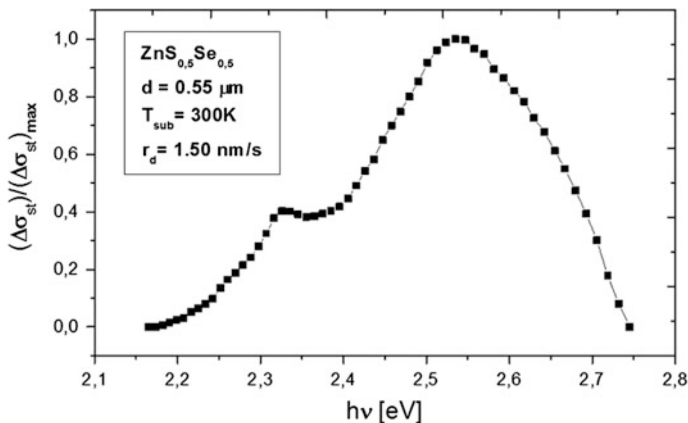

Fig. 4.23 Spectral dependence of photoconductivity of $ZnS_{0.5}Se_{0.5}$ thin films (T = 300 K, R_s = 47 MΩ, U = 180 V, ν = 12.5 Hz)

Figure 4.24 presents the photoluminescence relaxation curve of a $ZnS_{0.5}Se_{0.5}$ thin films. Excitation was performed with a molecular N_2 laser (λ_{ex} = 0.337 μm, P = 1.60 kW, $\Delta t = 10^{-8}$ s, f = 25 Hz) at the temperature of 78 K. The $J_{FL}(0)$ value is called stationary value of photoluminescence and the $J_{FL}(rem)$ is the residual value of luminescence.

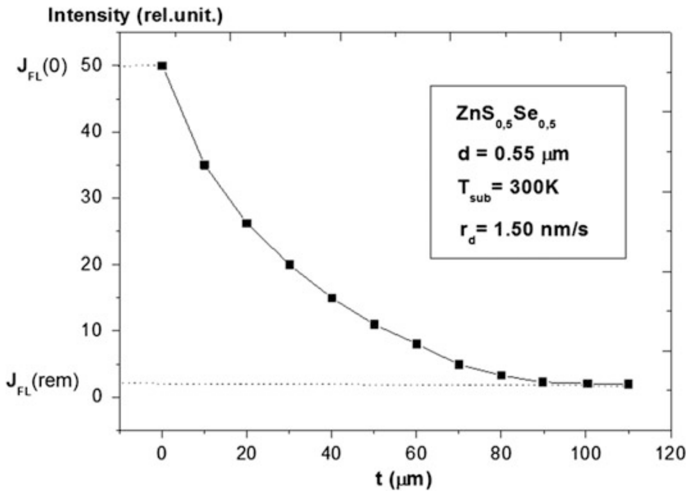

Fig. 4.24 Photoluminescence relaxation curve a $ZnS_{0.5}Se_{0.5}$ thin film

The lifetime of charge carriers can be determined according the relationship

$$\tau = \frac{t_2 - t_1}{ln\frac{J_{FL1}}{J_{FL}(0)} - ln\frac{J_{FL_2}}{J_{FL}(0)}}, \tag{4.20}$$

where J_{FL1} represents the stationary photoluminescence of the sample at time point t_1 and J_{FL2} is the stationary photoluminescence of the sample at time point t_2.

The dependence $ln(J_{FL}/J_{FL}(0)) = f(t)$ plotted for the same $ZnS_{0.5}Se_{0.5}$ sample si shown in Fig. 4.25. The relaxation time calculated from the slope of the linear

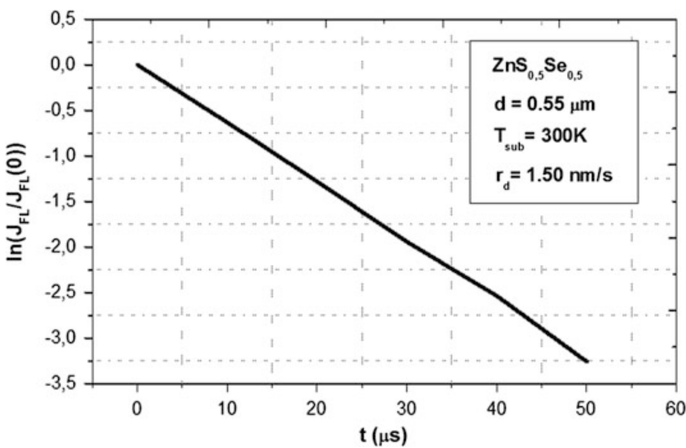

Fig. 4.25 Dependence $\ln(J_{FL}/J_{FL}(0)) = f(t)$ for a Zn $_{0.5}Se_{0.5}$ thin film

segment is equal to 15.38 μs. This value, as well as those obtained from of photoconductivity relaxation curves (Fig. 4.22) are in good agreement with those obtained by Şeikman and Şik [17] for ZnSe crystals.

The photoluminescence spectra of ZnS_xSe_{1-x} thin films were also investigated at the temperature of 78 K. The layers were obtained by vacuum thermal evaporation on glass substrates. $AuCl_2$ electrodes were deposited on layers at 1 mm distance from each other, and the samples were cooled to liquid nitrogen temperature. The photoluminescence excitation density was around 10^5 W/cm^2. The photoluminescence spectral dependence of $ZnS_{0.5}Se_{0.5}$ thin film measured at 78 K is presented in Fig. 4.26. The quantity Σ_{fL} is called relative spectral sensitivity of photoluminescence. The curve has a single peak, which is located approximately at 2.01 eV. Taking into account this value, we can determine the position of recombination centers as the difference between the width of the band gap (E_g = 3.05 eV) [3–6] and the value of 2.01 eV. Thus, one can conclude that the energy level of recombination centers in the $ZnS_{0.5}Se_{0.5}$ thin films is localized at a distance of 1.04 eV from the top edge of valence band.

Gaşin et al. [18] observed a respective peak in ZnSe crystals annealed in a Zn melt and then cooled to liquid nitrogen temperature. They assumed that the appearance of this band is related to $Zn_i^+ \rightarrow V_{Zn}$ radiative transitions. The activation energy of zinc vacancies is about 0.93 eV.

Other results are related to thermoluminescence of ZnS_xSe_{1-x} thin films. The excitation of luminescence centers was performed by ultraviolet radiation at T < 77 K. The excited electrons and holes are trapped at different energy levels in the band gap. With increasing temperature, release of "thermal" electrons from traps occurs. After a certain period of time, the free electrons either recombine on levels of recombination or are captured again in traps. Both processes are accompanied by emission of light radiation, called thermoluminescence.

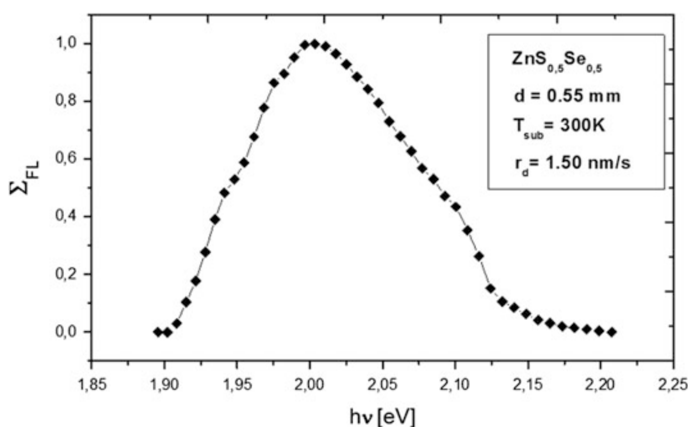

Fig. 4.26 Photoluminescence spectral dependence of a $ZnS_{0.5}Se_{0.5}$ thin film (λ_{ex} = 0.337 μm, T = 77 K, ν = 25 Hz)

The thermoluminescence parameters are [18]:

(a) the temperature at which thermoluminescence intensity is maximum (T_{max});
(b) the half-width of the thermoluminescence band (δ), equal to the difference $T_2{-}T_1$ for which thermoluminescence intensity is equal to half the maximum value;
(c) the surface area (S) limited by the curve $J_{TL} = f \quad (T)$and the axis of temperatures.

Vaksman and Serdiuk [19] deduced a formula for calculating the ionization energy of traps by using the parameters listed above. One can distinguish two cases:

(a) the case of *linear kinetics*

$$E_t = \frac{2k_B T_{max}}{\delta} \tag{4.21}$$

(b) the case of *quadratic kinetics*

$$E_t = \frac{4k_B T_{max}}{\delta}, \tag{4.22}$$

where $k_B = 8.6172 \times 10^{-5}$ (eV/K) is the Boltzmann constant.

Figure 4.27 presents the spectral dependence of thermoluminesce an $ZnS_xSe_{1\text{-}x}$ thin films. The curve has two peaks: the first, most intense one, appears at

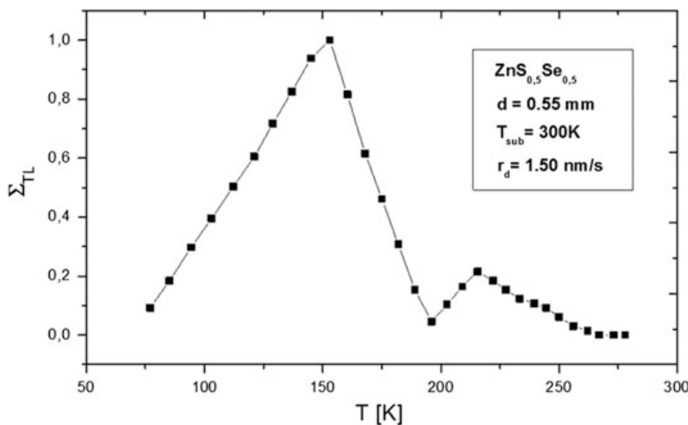

Fig. 4.27 Spectral dependence of thermoluminescence a $ZnS_{0.5}Se_{0.5}$ thin film (λ_{ex} = 0.337 μm, T = 77 K, ν = 25 Hz)

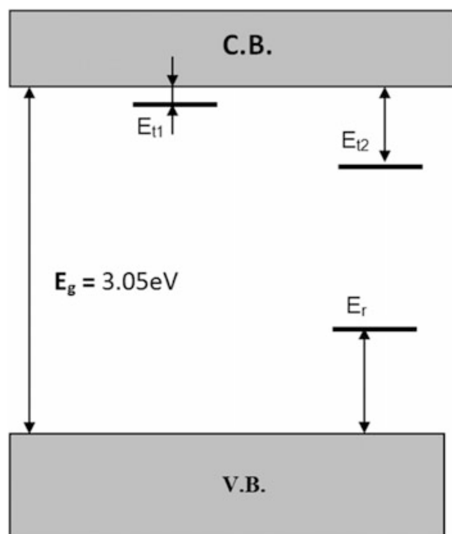

Fig. 4.28 Trapping levels and the level of localization of recombination centers from the band gap of $ZnS_{0.5}Se_{0.5}$ thin films

T_{max} = 153 K, and the second is situated at T_{max} = 216 K. One can observe that the low temperature part is higher than the high temperatures part for the first maximum (*linear kinetics*), while it is vice versa for the second maximum (*kinetic quadratic*). The E_t values calculated according to (4.18) and (4.19) equal to 0.062 and 0.44 eV for the frist and the second maximum, respectively.

A model can be proposed for the location of recombination and trapping levels in the band gap of of $ZnS_{0.5}Se_{0.5}$ thin films (Fig. 4.28) on the basis of thermoluminescence (Fig. 4.27) and photoluminescence (Fig. 4.26) spectra. The trapping levels are situated at 0.062 eV (E_{t1}) and 0.44 eV (E_{t2}) below the bottom of the conduction band, while the recombination centers are locallized at 0.93 eV (E_r) above the top edge of the valence band.

4.7 Conclusions

1. ZnS_xSe_{1-x} thin films (x = 0, 0.2, 0.4, 0.5, 0.6, 0.8, 1.0) with a thickness between 0.2 and 1.0 μm were prepared by thermal evaporation using the quasi closed volume technique.
2. The crystalline structure of layers was investigated by X-ray diffraction. It has been found that the layers are polycrystalline and have a cubic structure of zinc blende type with a large crystallite orientation of the planes (111) parallel to the surface of the substrate.
3. The cubic lattice parameter calculated from diffractograms is between a = 5.658–5.406 Å, the interplanar distance equals d_{111} = 3.270–3.120 Å, and the crystallite size is D = 3.750–2.435 Å. These values are in good agreement with prevuiously reported data.

4. The surface morphology of the polycrystalline ZnS_xSe_{1-x} thin films has been studied by scanning electron microscopy. The average crystallite size determined from the SEM images ranges between 3.6 and 2.2 Å.
5. The thermal activation energy determined from the dependencies $ln\sigma = f(10^3/T)$ is between 0.43–1.89 eV (for $T > 300$ K) and 0.132–0.403 eV (for $T < 300$ K). The mechanism of electron transport in polycrystalline ZnS_xSe_{1-x} thin films is explined on the basis of Efros-Shklovskii and Mott models.
6. The current-voltage characteristics of the In–ZnS_xSe_{1-x}–In systems plotted in Schottky coordinates proved to be linear. By extrapolating the linear segment of the $lnJ = f(U^{1/2})$ curve for $\sqrt{U} \rightarrow 0$, the height of the barrier potential at the metal-semiconductor interface was determined. The determined values for the Φ_0 are in agreement with those found for the ZnSe and ZnS crystals.
7. Transmission, reflection and absorption spectra have been investigated for polycrystalline ZnS_xSe_{1-x} thin films. It has been found that in the wavelength range of 380–1100 nm the reflectance does not exceed 0.5 %, and the transmission coefficient is in the range of 75–97 %.
8. The band gap width values determined from the reflection and absorption spectra (E_g = 2.65–3.5 eV) are in good agreement with the respective values for the bulk crystals.
9. The refractive index of polycrystalline ZnS_xSe_{1-x} thin films was determined from transmission spectra using the "envelope" method proposed by Swanepoel. It was found that the refractive index decreases with increasing the layer thickness, and it increases after the thermal treatment. A single oscillator model was used for explanation of the normal dispersion of the refractive index.
10. The lifetime (τ) of nonequilibrium charge carriers was calculated from the relaxation curves of photoconductivity and photoluminescence of ZnS_xSe_{1-x} of thin films. It was established that the value of relaxation time decreases with increasing the sample temperature.
11. The location of energy levels of recombination centers was determined from photoluminescence spectra, and the ionization energy of traps was calculated from the thermoluminescence spectra of ZnS_xSe_{1-x} thin films.

References

1. M.S. Shinde, P.B. Ahirrao, I.J. Patil, R.S. Patil, Studies of nanocristalline ZnSe thin films prepared by modified chemical bach deposition method. Indian J. Pure Appl. Phys. **49**, 765–768 (2011)
2. Y. Sirotin, M. Shaskolskaya, *Fundamental of Crystal Physics* (Mir Publishers, Moscow, 1982)
3. Y.P. Venkata Subbaiah, K.T. Ramakrishna Reddy, Structural behaviour of ZnS_xSe_{1-x} films deposited by close-spaced evaporation. Mater. Chem. Phys. **92,** 448–452 (2005)
4. M. Ambrico, G. Perna, D. Smaldone, C. Spezzacatena, V. Stagno, V. Capozzi, Structural and optical parameters of ZnS_xSe_{1-x} films deposited on quartz substrates by laser ablation. Semicond. Sci. Technol. **13**, 1446–1455 (1998)

5. Y.P. Venkata Subbaiah, P. Prathap, K.T.R. Reddy, D. Mangalaraj, K. Kim, Yi. Junsin, Growth and characterization of ZnS_xSe_{1-x} films deposited by close-spaced evaporation. J. Phys. D Appl. Phys. **40**, 3683–3688 (2007)
6. A. Ganguly, S. Chaudhury, A.K. Pal, Synthesis of ZnS_xSe_{1-x} ($0 < \mathbf{x} < 1$) nanocrystalline thin films by high-pressure sputtering. J. Phys. D Appl. Phys. **34**, 506–513 (2001)
7. D.D. Nedeoglo, A.V. Simaşkevici, *Elektriceskie i liuminisţentnâe svoistva selenida ţinka*, Chişinău, (ed.) "Ştiinţa", 1984
8. R. Bhargava (ed.), *Properties of Wide Bandgap II–VI Semiconductors* (Inspection, London, 1997)
9. M. Jain (ed.), *II–VI Semiconductor Compounds* (World Scientific, Singapore, 1993)
10. B.I. Shklovsky, A.L. Efros, *Electronic Properties of Doped Semiconductors* (Nauka, Moscow, Russia, 1979)
11. H.E. Bennett, J.M. Bennett, in *Physics of Thin Films* vol. 4, eds. by G.Hass, R.E.Thun (Academic Press, New York, 1987), p.1–96
12. R. Swanepoel, Determination of the thickness and optical constants of amorphous silicon. J. Phys. E: Sci. Instrum. **16**, 1214–1222 (1983)
13. R. Swanepoel, Determination of the surface roughness and optical constants of inhomogeneous amorphous silicon films. J. Phys. E: Sci. Instrum. **17,** 896–903 (1984)
14. L. Meng, M. Andritschky, M.P. dos Santos, The effect of substrate temperature on the properties of d.c. reactive magnetron sputtered titanium oxide films. Thin Solid Films **223**, 242–247 (1993)
15. T.S. Moss, in *Handbook on Semiconductors, Optical Properties of Semiconductors*, vol.2, ed. by M.Balkanski (Elsevier, Amsterdam, 1994)
16. G. Harbeke, *Polycrytalline Semiconductors: Physical Properties and Applications* (Springer, Berlin, 1985)
17. М.Я. Шейнкман, А.Я. Шик, Долговременные релаксации и остаточная проводимость в полупроводниках. Физика и техника полупроводников **10**(2), 209 (1976)
18. Гашин, П.А., Иванова, Г.Н., Матвеева, Т.Л. и др. *Фотолюминесценция монокристаллов ZnSe: Al*, Физ. и техн. Полупроводников, 1981, т.15, №9, с. 1841–1844
19. V.V. Serdiuk, Iu.F. Vaksman, *Liuminisţenţia poluprovodnikov*, Kiev-Odessa, Izd-vo "Vâşşaia şkola", 1988